The Fifteenth International Symposium on Artificial Life and Robotics 2010 (AROB 15th '10),
B-Con Plaza, Beppu,Oita, Japan, February 4-6, 2010

Digital RAC with Disturbance Observer for Underwater Vehicle-Manipulator Systems

Shinichi Sagara Takashi Yatoh Tomoaki Shimozawa
Department of Control Engineering, Kyushu Institute of Technology
Tobata, Kitakyushu 804-8550, Japan
E-mail: sagara@cntl.kyutech.ac.jp

Abstract

Most of control methods of Underwater Vehicle-Manipulator Systems (UVMS) are based on the computed torque method that is used for underwater robotic vehicles. We have proposed a Resolved Acceleration Control (RAC) method for UVMS. In this paper, we propose a disturbance compensation control method for both vehicle and manipulator based on the RAC method. Experimental results using an underwater robot with vertical planar 2-link manipulator show that the proposed control method has good control performance.

1 Introduction

Most of the control methods of Underwater Vehicle-Manipulator Systems (UVMS) [1–5] are based on the computed torque method that is used for Underwater Robotic Vehicles [6]. Since the computed torque method only uses joint-space errors, the control performance of the end-effector of the manipulator depends on the vehicle control performance. Therefore, if the acceleration and velocity relations between the end-effector and joints are inaccurate or the control performance of the vehicle is not better, good control performance of the end-effector cannot be obtained.

We have proposed a Resolved Acceleration Control (RAC) method with position and velocity feedbacks both of the vehicle and the end-effector [7]. In general, added mass, added moment of inertia and drag coefficient are used constant value that depends on the shape of the robots. Our proposed method described above can reduce the influence of hydrodynamic force by position and velocity feedbacks. Moreover, to obtain higher control performance, we have proposed a disturbance compensation control method based on the RAC method [8]. In this control method, the influence of hydrodynamic force with respect to the vehicle is treated as a disturbance.

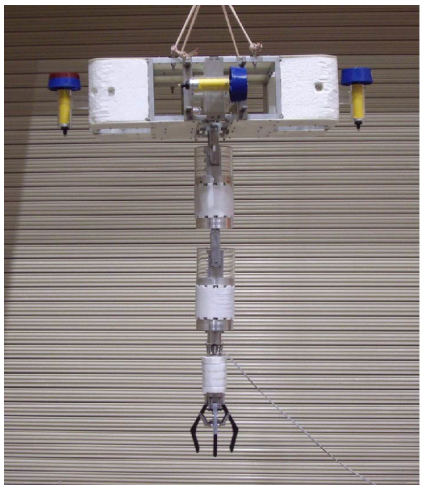

Fig. 1 2-link underwater robot

In this paper, we propose a disturbance compensation control method for both vehicle and manipulator. To verify the effectiveness of the digital RAC method with disturbance observer, experiments using an underwater robot with vertical planar 2-link manipulator shown in Fig. 1 are performed. From the experimental results, we show that the proposed control method has good control performance.

2 Modeling [7]

The UVMS model used in this paper is shown in Fig. 2. It has a robot base (vehicle) and an n-DOF manipulator. Symbols are defined as follows:

- n : number of joint
- Σ_I : inertial coordinate frame
- Σ_i : link i coordinate frame ($i = 0,\ 1,\ 2,\ \cdots,\ n$; link 0 means vehicle)
- ${}^I\boldsymbol{R}_i$: coordinate transformation matrix from Σ_i to Σ_I
- $\boldsymbol{p}_e$: position vector of end-effector
- $\boldsymbol{p}_i$: position vector of origin of Σ_i

$\boldsymbol{r}_i$: position vector of gravity center of link i
ϕ_i : relative angle of joint i
$\boldsymbol{\psi}_0$: roll-pitch-yaw attitude vector of Σ_0
$\boldsymbol{\psi}_e$: roll-pitch-yaw attitude vector of end-effector
$\boldsymbol{\omega}_0$: angular velocity vector of Σ_0
$\boldsymbol{\omega}_e$: angular velocity vector of end-effector
$\boldsymbol{\phi}$: relative joint angle vector $(= [\phi_1, \cdots, \phi_n]^T)$
$\boldsymbol{k}_i$: unit vector indicating a rotational axis of joint i
m_i : mass of link i
$\boldsymbol{M}_{a_i}$: added mass matrix of link i
$\boldsymbol{I}_i$: inertia tensor of link i
$\boldsymbol{I}_{a_i}$: added inertia tensor of link i
$\boldsymbol{x}_0$: position and attitude vector of Σ_0 $(= [\boldsymbol{r}_0^T, \boldsymbol{\psi}_0^T]^T)$
$\boldsymbol{x}_e$: position and attitude vector of end-effector $(= [\boldsymbol{p}_e^T, \boldsymbol{\psi}_e^T]^T)$
$\boldsymbol{v}_0$: linear and angular vector of Σ_0 $(= [\dot{\boldsymbol{r}}_0^T, \boldsymbol{\omega}_0^T]^T)$
$\boldsymbol{v}_e$: linear and angular vector of end-effector $(= [\dot{\boldsymbol{p}}_e^T, \boldsymbol{\omega}_e^T]^T)$
$\boldsymbol{E}_j$: $j \times j$ unit matrix

The tilde operator stands for a cross product such that $\tilde{\boldsymbol{r}}\boldsymbol{a} = \boldsymbol{r} \times \boldsymbol{a}$. All position and velocity vectors are defined with respect to Σ_I

First, for the model shown in Fig. 2 the following kinematic and momentum equations can be obtained:

$$\boldsymbol{v}_e = \boldsymbol{A}\boldsymbol{v}_0 + \boldsymbol{B}\dot{\boldsymbol{\phi}}, \tag{1}$$

$$\boldsymbol{s} = [\boldsymbol{\eta}^T, \boldsymbol{\mu}^T]^T = \boldsymbol{C}\boldsymbol{v}_0 + \boldsymbol{D}\dot{\boldsymbol{\phi}} \tag{2}$$

where

$$\boldsymbol{A} = \begin{bmatrix} \boldsymbol{E}_3 & -(\tilde{\boldsymbol{p}}_r - \tilde{\boldsymbol{r}_0}) \\ \boldsymbol{0} & \boldsymbol{E}_3 \end{bmatrix}, \quad \boldsymbol{B} = [\boldsymbol{b}_1\ \boldsymbol{b}_2\ \cdots\ \boldsymbol{b}_n],$$

$$\boldsymbol{C} = \begin{bmatrix} \sum_{i=0}^{n} \boldsymbol{M}_{T_i} & -\sum_{i=1}^{n} \boldsymbol{M}_{T_i}\tilde{\boldsymbol{r}}_{0i} \\ \sum_{i=0}^{n} \tilde{\boldsymbol{r}}_{0i}\boldsymbol{M}_{T_i} & \sum_{i=0}^{n} \{\boldsymbol{I}_{T_i} - \tilde{\boldsymbol{r}}_{0i}\boldsymbol{M}_{T_i}\tilde{\boldsymbol{r}}_{0i}\} \end{bmatrix},$$

$$\boldsymbol{D} = \begin{bmatrix} \boldsymbol{d}_{11} & \boldsymbol{d}_{11} & \cdots & \boldsymbol{d}_{1n} \\ \boldsymbol{d}_{21} & \boldsymbol{d}_{21} & \cdots & \boldsymbol{d}_{2n} \end{bmatrix},$$

$$\boldsymbol{b}_i = \begin{bmatrix} \{\tilde{\boldsymbol{k}}_i(\boldsymbol{p}_r - \boldsymbol{p}_i)\}^T & \boldsymbol{k}_i^T \end{bmatrix}^T, \ \boldsymbol{r}_{0i} = \boldsymbol{r}_i - \boldsymbol{r}_0,$$

$$\boldsymbol{d}_{1i} = \sum_{j=i}^{n} \boldsymbol{M}_{T_i}\tilde{\boldsymbol{k}}_i(\boldsymbol{r}_j - \boldsymbol{p}_i),$$

$$\boldsymbol{d}_{2i} = \sum_{j=i}^{n} \boldsymbol{I}_{T_j}\boldsymbol{k}_i + \tilde{\boldsymbol{r}}_{0j}\boldsymbol{M}_{T_j}\tilde{\boldsymbol{k}}_i(\boldsymbol{r}_j - \boldsymbol{p}_i)$$

and, $\boldsymbol{\eta}$ and $\boldsymbol{\mu}$ are a linear and an angular momentum of the robot.

Next, to obtain the dynamic equation of UVMS, hydrodynamic the drag and lift forces are necessary.

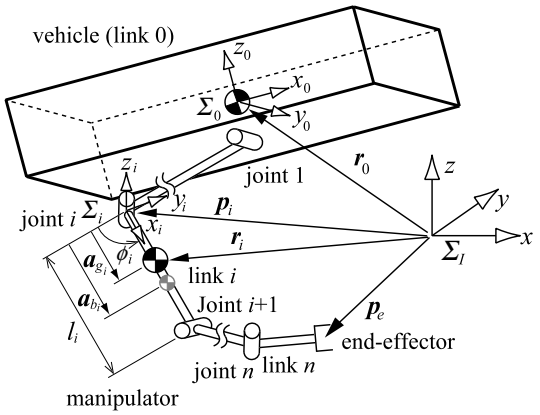

Fig. 2 n-link underwater robot model

The drag force and moment of joint i can be generally represented as follows [9]:

$$\boldsymbol{f}_{d_i} = \frac{\rho}{2} C_{D_i} D_i{}^I\boldsymbol{R}_i \int_0^{l_i} ||\boldsymbol{w}_i||\boldsymbol{w}_i dx_i, \tag{3}$$

$$\boldsymbol{t}_{d_i} = \frac{\rho}{2} C_{D_i} D_i{}^I\boldsymbol{R}_i \int_0^{l_i} \hat{\boldsymbol{x}}_i \times ||\boldsymbol{w}_i||\boldsymbol{w}_i dx_i \tag{4}$$

where

$$\boldsymbol{w}_i = \begin{bmatrix} 0 & \boldsymbol{0} \\ \boldsymbol{0} & \boldsymbol{E}_2 \end{bmatrix} {}^i\boldsymbol{R}_I \left(\dot{\boldsymbol{r}}_i + \tilde{\boldsymbol{\omega}}_i\hat{\boldsymbol{x}}_i\right), \quad \hat{\boldsymbol{x}}_i = \begin{bmatrix} x_i & 0 & 0 \end{bmatrix}^T.$$

and ρ is the fluid density, C_{d_i} is the drag coefficient of link i, D_i is the width of link i, l_i is the length of link i,

In the similar manner, the gravitational and buoyant forces acting link i are described as follows:

$$\boldsymbol{f}_{g_i} = (\rho V_i - m_i)\boldsymbol{g}, \tag{5}$$

$$\boldsymbol{t}_{g_i} = (\tilde{\boldsymbol{a}}_{b_i}\rho V_i - \tilde{\boldsymbol{a}}_{g_i} m_i)\boldsymbol{g} \tag{6}$$

where $\boldsymbol{a}_{g_i}$ is the position vector from joint i to gravity center of link i, $\boldsymbol{a}_{b_i}$ is the position vector from joint i to buoyancy center of link i, V_i is the volume of link i, $\boldsymbol{g}$ is the gravitational acceleration vector.

Considering the hydrodynamic forces described above and using the Newton-Euler formulation, the following equation of motion can be obtained [5]:

$$\boldsymbol{M}(\boldsymbol{q})\dot{\boldsymbol{\zeta}} + \boldsymbol{b}_C(\boldsymbol{q}, \boldsymbol{\zeta}) + \boldsymbol{f} = \boldsymbol{u} \tag{7}$$

where $\boldsymbol{q} = [\boldsymbol{x}_0^T, \boldsymbol{\phi}^T]^T$ and $\boldsymbol{\zeta} = [\dot{\boldsymbol{v}}_0^T, \dot{\boldsymbol{\phi}}^T]^T$, $\boldsymbol{M}$ is the inertia matrix including the added mass $\boldsymbol{M}_{a_i}$ and inertia $\boldsymbol{I}_{a_i}$, $\boldsymbol{b}_C$ is the vector of Coliolis and centrifugal forces, $\boldsymbol{f}$ is the vector consisting of the drag, gravitational and buoyant forces and moments, $\boldsymbol{u} = [\boldsymbol{f}_0^T, \boldsymbol{\tau}_0^T, \boldsymbol{\tau}_m^T]^T$, $\boldsymbol{f}_0$ and $\boldsymbol{\tau}_0$ are the force and torque vectors of vehicle, $\boldsymbol{\tau}_m$ is the joint torque vector of manipulator.

Furthermore, the relationship between $\boldsymbol{\omega}_*$ and $\dot{\boldsymbol{\psi}}_* = [\psi_{r_*},\ \psi_{p_*},\ \psi_{y_*}]^T$ $(* = 0,\ e)$ is described as

$$\boldsymbol{\omega}_* = \boldsymbol{S}_{\boldsymbol{\psi}_*}\dot{\boldsymbol{\psi}}_* \tag{8}$$

where

$$\boldsymbol{S}_{\boldsymbol{\psi}_*} = \begin{bmatrix} \cos\psi_{p_*}\cos\psi_{y_*} & -\sin\psi_{y_*} & 0 \\ \cos\psi_{p_*}\sin\psi_{y_*} & \cos\psi_{y_*} & 0 \\ \sin\psi_{p_*} & 0 & 1 \end{bmatrix}.$$

Thus the relationship between $\dot{\boldsymbol{q}}$ and $\dot{\boldsymbol{\zeta}}$ is described as

$$\dot{\boldsymbol{\zeta}} = \boldsymbol{S}_q\dot{\boldsymbol{q}} \tag{9}$$

where $\boldsymbol{S}_q = \text{blockdiag}\{\boldsymbol{S}_{v\boldsymbol{\psi}_0},\ \boldsymbol{E}_n\}$ and $\boldsymbol{S}_{v\boldsymbol{\psi}_*} = \text{blockdiag}\{\boldsymbol{E}_3,\ \boldsymbol{S}_{\boldsymbol{\psi}_*}\}$ $(* = 0,\ e)$.

3 Configuration of Control System

3.1 Digital RAC [7]

Differentiating Eqs. (1) and (2) with respect to time, the following equation can be obtained:

$$\boldsymbol{W}(t)\boldsymbol{\alpha}(t) = \beta(t) + \boldsymbol{\gamma}(t) - \dot{\boldsymbol{W}}(t)\boldsymbol{\zeta}(t) \tag{10}$$

where

$$\boldsymbol{W} = \begin{bmatrix} \boldsymbol{C}+\boldsymbol{E}_6 & \boldsymbol{D} \\ \boldsymbol{A} & \boldsymbol{B} \end{bmatrix},\quad \boldsymbol{\alpha} = \dot{\boldsymbol{\zeta}},\quad \beta = \begin{bmatrix} \dot{\boldsymbol{v}}_0 \\ \dot{\boldsymbol{v}}_e \end{bmatrix},\quad \boldsymbol{\gamma} = \begin{bmatrix} \dot{\boldsymbol{s}} \\ \boldsymbol{0} \end{bmatrix}$$

and $\dot{\boldsymbol{s}}$ is the external force, including hydrodynamic force and thrust of the thruster which act on the base.

Discretizing Eq. (10) by a sampling period T, and applying $\beta(k)$ and $\dot{\boldsymbol{W}}(k)$ to the backward Euler approximation, we have

$$\begin{aligned}\boldsymbol{W}(k)\boldsymbol{\alpha}(k-1) = \frac{1}{T}&\left[\boldsymbol{v}(k) - \boldsymbol{v}(k-1) + T\boldsymbol{\gamma}(k)\right. \\ &\left. - \{\boldsymbol{W}(k) - \boldsymbol{W}(k-1)\}\boldsymbol{\zeta}(k)\right]\end{aligned} \tag{11}$$

where $\boldsymbol{v} = [\boldsymbol{v}_0^T\ \boldsymbol{v}_e^T]^T$. Note that a computational time delay is introduced into Eq. (11), and the discrete time kT is abbreviated to k.

For Eq. (11), the desired acceleration and velocity are defined as follows:

$$\begin{aligned}\boldsymbol{\alpha}_d(k) = \frac{1}{T}&\boldsymbol{W}^\sharp(k)\left[\boldsymbol{v}_d(k+1) - \boldsymbol{v}_d(k)\right. \\ &\left. + \boldsymbol{\Lambda}\boldsymbol{e}_v(k) + T\boldsymbol{\gamma}(k)\right],\end{aligned} \tag{12}$$

$$\boldsymbol{\nu}_d(k) = \frac{\boldsymbol{S}_{0e}}{T}\left\{\boldsymbol{x}_d(k) - \boldsymbol{x}_d(k-1) + \boldsymbol{\Gamma}\boldsymbol{e}_x(k-1)\right\} \tag{13}$$

where $\boldsymbol{e}_v(k) = \boldsymbol{v}_d(k) - \boldsymbol{v}(k)$, $\boldsymbol{e}_x(k) = \boldsymbol{x}_d(k) - \boldsymbol{x}(k)$, $\boldsymbol{S}_{0e} = \text{blockdiag}\{\boldsymbol{S}_{\nu\psi_0},\ \boldsymbol{S}_{\nu\psi_e}\}$, and $\boldsymbol{W}^\sharp$ is the pseudoinverse of $\boldsymbol{W}$, i.e. $\boldsymbol{W}^\sharp = \boldsymbol{W}^T(\boldsymbol{W}\boldsymbol{W}^T)^{-1}$, $\boldsymbol{x}_d$ is the desired value of $\boldsymbol{x} = [\boldsymbol{x}_0^T,\ \boldsymbol{x}_e^T]^T$, $\boldsymbol{\Lambda} = \text{diag}\{\lambda_i\}$ and $\boldsymbol{\Gamma} = \text{diag}\{\gamma_i\}$ $(i = 1, \cdots, 12)$ are the velocity and the position feedback gain matrices.

From Eqs. (11), (12) and (13), if λ_i and γ_i are selected to satisfy $0 < \lambda_i < 1$ and $0 < \gamma_i < 1$, respectively, and the convergence of the acceleration error, $\boldsymbol{e}_\alpha(k) = \boldsymbol{\alpha}_d(k) - \boldsymbol{\alpha}(k)$, tends to zero as k tends to infinity, then the convergence of $\boldsymbol{e}_\nu(k)$ and $\boldsymbol{e}_x(k)$ to zero as k tends to infinity can be ensured.

3.2 Disturbance compensation

From the viewpoint of underwater robot control, parameters and coefficients of hydrodynamic models are generally used as constant values that depends on the shape of the robots [6]. Here, to obtain higher control performance, the influence of hydrodynamic modeling error is treated as a disturbance and a disturbance compensation method is introduced.

The nominal model of $\boldsymbol{M}$ in Eq. (7) is defined as $\bar{\boldsymbol{M}}$. In $\bar{\boldsymbol{M}}$ the added mass and moment of inertia and the drag coefficient are constant. Furthermore, the following force is similarly defined:

$$\boldsymbol{f}_t = \bar{\boldsymbol{b}}_C(\boldsymbol{q},\ \boldsymbol{\zeta}) + \bar{\boldsymbol{f}} \tag{14}$$

where $\bar{\boldsymbol{b}}_C$ and $\bar{\boldsymbol{f}}$ are nominal of $\boldsymbol{b}_C$ and $\boldsymbol{f}$, respectively.

When the modeling error with respect to the hydrodynamic force regards the disturbance, the following estimated value can be obtained:

$$\hat{\boldsymbol{f}}_E = F(s)\left(\boldsymbol{u} - \bar{\boldsymbol{M}}\boldsymbol{\alpha}_d - \boldsymbol{f}_t\right) \tag{15}$$

where $F(s) = 1/(T_f s + 1)$ is a low pass filter with a time constant T_f.

Using Eqs. (14) and (15) we have the following control input of the robot:

$$\boldsymbol{u} = \bar{\boldsymbol{M}}\boldsymbol{\alpha}_d + \boldsymbol{f}_t + \hat{\boldsymbol{f}}_E \tag{16}$$

The configuration of the disturbance compensation is shown in Fig. 3(a). In Fig. 3(a) $\boldsymbol{f}_L$ is the external force. Furthermore, for the digital control system, Fig. 3(a) can be descretized to Fig. 3(b) [10] where $h = e^{-T_f/T}$.

4 Experiments

In this section, experiments of catching an object using the robot shown in Fig. 1 are done to verify the effectiveness of the proposed control method. Physical parameters of the robot are shown in Table 1.

Fig. 4 shows a configuration of an experimental system. A robot has a 2-DOF manipulator with joints that are actively rotated by torque-control-type

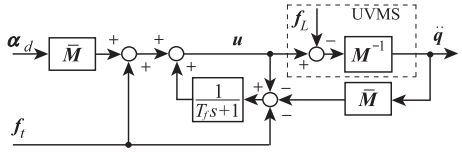

(a) analog

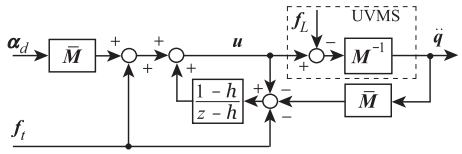

(b) digital

Fig. 3 Disturbance compensation

Table 1 Physical parameters of underwater robot

	Base	Link 1	Link 2
Mass [kg]	20.82	4.65	5.29
Moment of inertia [kg m^2]	1.33	0.075	0.26
Link length (x axis) [m]	0.2	0.35	0.64
Link length (z axis) [m]	0.81	-	-
Link width [m]	0.42	0.13	0.13
Added mass(x) [kg]	72.7	0.35	0.35
Added mass(z) [kg]	6.28	3.31	3.92
Added moment of inertia [kg m^2]	1.05	0.06	0.076
Drag coefficient(x)	1.2	0	0
Drag coefficient(z)	1.2	1.0	1.0

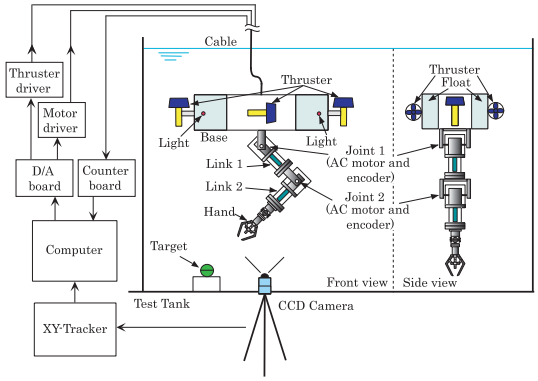

Fig. 4 Configuration of underwater robot system

servo actuators consisting of AC servo motors and incremental-type encoders. Four 40[W] thrusters are attached to the vertical and horizontal direction on the robot base to provide propulsion for controlling the position and attitude angle of the base.

Experiments are carried out under the following condition. The object is a ball that is 0.4[kg] in weight and 0.085[m] in diameter. The sampling period is $T = 1/60$[s], the time constant of the low-pass filter is $T_f = 1$[s] for the base and $T_f = 0.2$[s] for the manipulator. The feedback gains are $\mathbf{\Lambda} = \mathrm{diag}\{0.01,\ 0.01,\ 0.03,\ 0.02,\ 0.02\}$ and $\mathbf{\Gamma} = \mathrm{diag}\{0.02,\ 0.02,\ 0.06,\ 0.005,\ 0.005\}$. Furthermore, the initial relative joint angles are $\phi_0 = -\pi/2$[rad], $\phi_1 = \pi/3$[rad] and $\phi_2 = -7\pi/18$[rad].

The desired position and attitude of the robot base is set up to the initial values. On the other hand, the desired position of the end-effector is set up the following procedure:

Action 1: Moving along a straight path from the initial position to the target.
Action 2: Catching the object keeping the position.
Action 3: Lifting up the object along the straight path.

The experimental results without and with the disturbance compensation are shown in Figs. 5 and 6, respectively. From Fig. 5, we can be seen that the robot cannot lift up the object because of the change of the physical parameter of the manipulator including the object. On the other hand, from Fig. 6, it can be seen that the base position and attitude errors become small values and the manipulator can lift up the object by using the disturbance compensation. Therefore, the control performance can be improved by using the disturbance compensation.

5 Conclusion

In this paper, we proposed a disturbance compensation control method for UVMS based on the RAC method. The experimental results showed the effectiveness of the proposed method.

References

[1] H. Maheshi *et al.*, "A Coordinated Control of an Underwater Vehicle and Robotic Manipulator", *J. Robotic Systems*, Vol. 8, No. 3, pp. 339 – 370, 1991.
[2] T. W. McLain *et al.*, "Experiments in the Coordinated Control of an Underwater Arm/Vehicle System", *Autonomous Robots 3*, Kluwer Academic Publishers, pp. 213 – 232, 1996.
[3] G. Antonelli *et al.*, "Tracking Control for Underwater Vehicle-Manipulator Systems with Velocity Estimation", *IEEE J. Oceanic Eng.*, Vol. 25, No. 3, pp. 399 – 413, 2000.
[4] N. Sarkar and T. K. Podder, "Coordinated Motion Planning and Control of Autonomous Underwater Vehicle-Manipulator Systems Subject to Drag Optimization", *IEEE J. Oceanic Eng.*, Vol. 26, No. 2, pp. 228 – 239, 2001.

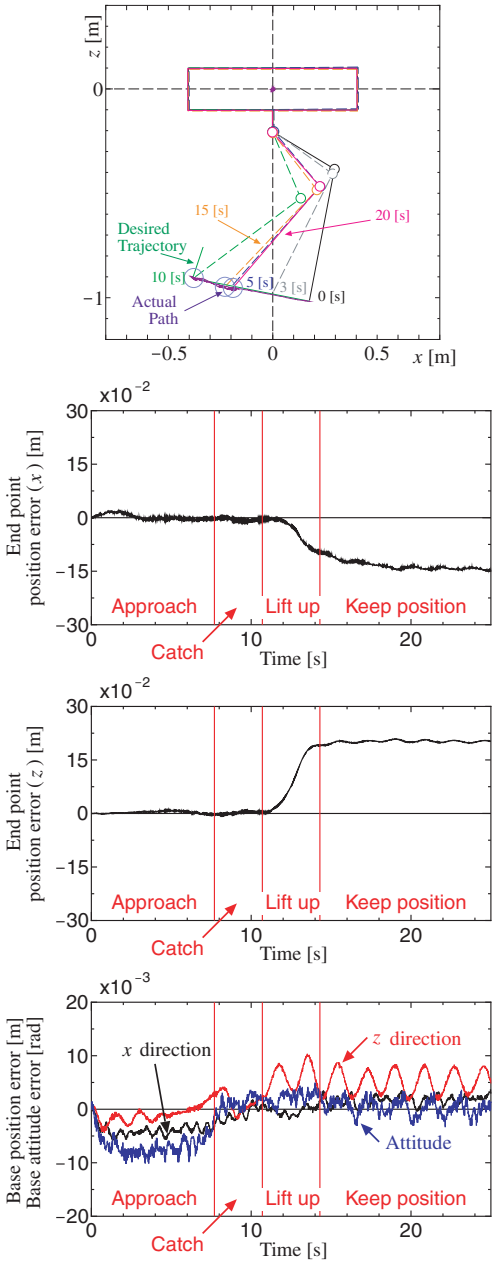

Fig. 5 Experimental result without compensation

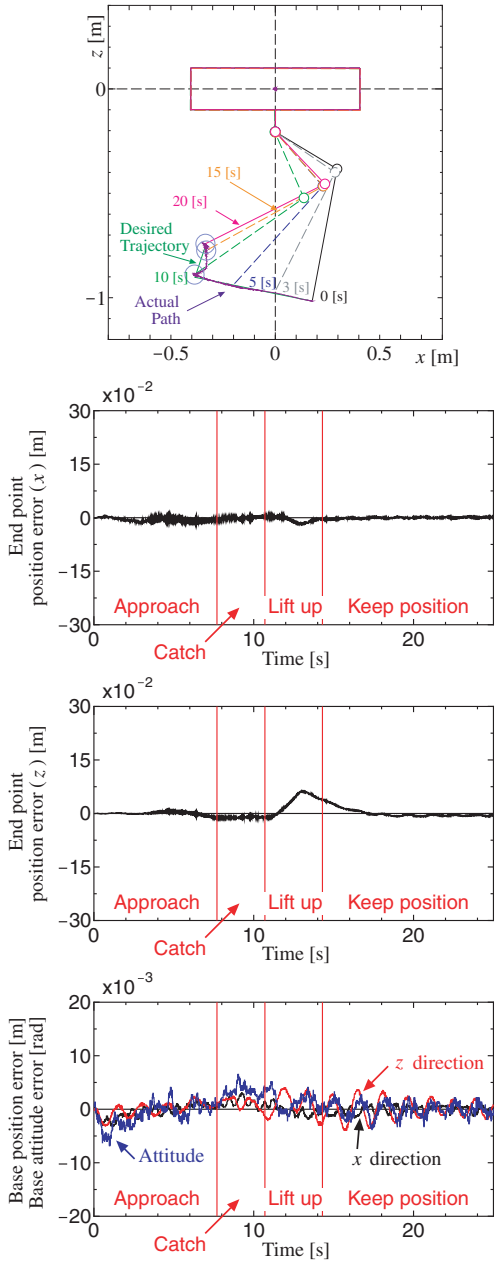

Fig. 6 Experimental result with compensation

[5] G. Antonelli, *Underwater Robotics*, Springer, pp. 1194–1206, 2003.
[6] T. I. Fossen, *Guidance and Control of Ocean Vehicles*, John Wiley & Sons, pp. 431–452, 1995.
[7] S. Sagara *et al.*,"Digital RAC for Underwater Vehicle-Manipulator Systems Considering Singular Configuration", *J. Artificial Life and Robotics*, Vol. 10, No. 2, pp. 106 – 111, 2006.
[8] T. Yatoh and S. Sagara, "Digital Type Disturbance Compensation Control of Underwater Vehicle-Manipulator Systems", *Proc. OCEANS'08 MTS/IEEE Kobe-Techno-Ocean'08*, Paper No. 071109-002, 2008.
[9] B. Lévesque and M. J. Richard, "Dynamic Analysis of a Manipulator in a Fluid Environment", *Int. J. Robot. Res.*, Vol. 13, No. 3, pp. 221 – 231, 1994.
[10] I. Godler, H. Honda and K. Ohnishi, "Design Guidelines for Disturbance Observer's Filter in Discrete Time", *Proc. 7th Int. Workshop on Advanced Motion Control*, pp. 390 – 395, 2002.